High nitrite concentration accelerates nitrite oxidising organism's death

Bing Liu, Mitsuharu Terashima, Nguyen Truong Quan, Nguyen Thi Ha, Le Van Chieu, Rajeev Goel and Hidenari Yasui

ABSTRACT

High nitrite is a known operation parameter to inhibit the biological oxidation of nitrite to nitrate. The phenomenon is traditionally expressed using a Monod-type equation with non-competitive inhibition, in which the reaction associated with the biomass growth is reduced when high nitrite is present. On the other hand, very high nitrite is also known to slay nitrifiers. To clarify the difference between the growth inhibition and the poisoning, cell counting for living microorganisms in the nitrite oxidiser-enriched activated sludge was conducted in batch conditions under various nitrite concentrations together with measurements of biomass chemical oxygen demand (COD) concentration and oxygen uptake rate. The experiments demonstrated that these measureable parameters were all decayed when nitrite concentration exceeded 100–500 mgN/L at pH 7.0 in the system, indicating that nitrite poisoning took place. Biomass growth was recognised in lower range of nitrite which was expressed with growth inhibition only. Based on the response, a kinetic model for the biological nitrite oxidation was developed with a modification of IWA ASM1. The model was further utilised to calculate a possibility to wash out nitrite oxidiser in the aeration tank where a part of the return activated sludge was exposed to high nitrite liquor in a side-stream partial nitritation reactor.

Key words | kinetic model, living bacteria staining, oxygen uptake rate, suppression of nitrite oxidiser

Bing Liu
Mitsuharu Terashima
Hidenari Yasui (corresponding author)
Faculty of Environmental Engineering,
The University of Kitakyushu,
1-1, Hibikino Wakamatsu, Kitakyushu,
Japan
E-mail: *hidenari-yasui@kitakyu-u.ac.jp*

Nguyen Truong Quan
Nguyen Thi Ha
Le Van Chieu
Department of Environmental Technology,
VNU University of Science,
334 Nguyen Trai, Thanh Xuan, Hanoi,
Vietnam

Rajeev Goel
Hydromantis Environmental Software Solutions,
Inc.,
407 King Street West, Hamilton, Ontario,
Canada

INTRODUCTION

Microbial growth rate is usually expressed using a Monod-type equation where concentrations of substrate, oxygen, nutrients, etc. are multiplied by the maximum specific growth rate (μ_{max}) as a set of dimensionless switching functions ($0 \leq \text{material}/(K_S + \text{material}) \leq 1$) with each individual half-saturation coefficient, K_S. In case of need to express the impact of inhibitory materials on the microbial reaction, dimensionless switching functions with inversed form (1–0) are also introduced. When high inhibitory material is present in the system, the specific growth rate (μ) is reduced in proportion to the infinite product ($\mu = \mu_{max} \times \Pi$(dimensionless switching functions)). To express the inhibition of nitrite for nitrite oxidising organism (NOO), Anthonisen *et al.* (1976) and Wett & Rauch (2003) selected a non-competitive type inhibition switching function, ($K_I/(K_I +$ nitrite)) with a half-saturation inhibition coefficient K_I. Focusing on the kinetic property to reduce the growth of NOO under high nitrite concentration, partial nitritation processes are being developed for the treatments of high strength ammonium-N wastewater (Manser *et al.* 2006; Wallenstein *et al.* 2006; Wu *et al.* 2016a). The concept of non-competitive inhibition is widely mentioned in various kinds of aerobic/anoxic biological systems (e.g. dissolved oxygen (DO) inhibition for denitrification) as well as anaerobic treatments (e.g. hydrogen inhibition of propionate degradation) (Batstone *et al.* 2002; Henze *et al.* 2000; Calderer *et al.* 2010; David and Peter 2016). Similarly, NOO's specific growth rate can be also suppressed under micro aerobic condition (low DO set point) (Chen *et al.* 2016). This growth control is adopted to develop simultaneous nitritation and Anammox reactions in the aeration tanks (known as main stream partial nitritation and Anammox process) where the nitrite concentration is too low to inhibit NOO (Wu *et al.* 2016b).

doi: 10.2166/wst.2018.272

Besides the above biostatic effects on microbial growth, when the toxic material is dosed to the system, microorganisms are inactivated. This phenomenon is commonly known as biocidal effect. Since the biocidal effect may be defined as an elevation of microbial death rate, this irreversible reaction can be classified as one of microbial decay processes. In this case, the total specific decay rate (b_{tot}) may be expressed as a summation of probability for each specific inactivation per unit time including the ordinary specific decay rate and the specific toxicity rates ($b_{tot} = \Sigma$) (specific inactivation rate). This is because the microbial decay is generally supposed to be a consequence of stochastic irreversible inactivation of the microorganisms that randomly happens over the population in the system, in which the mathematical formula is eventually expressed with a first-order reaction in terms of microorganism concentration (Weibull 1952).

However, the concept to map the growth inhibition and toxicity to the corresponding unit processes is still hypothetical at present and not clearly understood due to lack of experimental evidence (Liu *et al.* 2013). In fact, unlike modelling growth inhibition, research to integrate ordinal decay with toxicity are limited in literature. In this regard, since nitrite simultaneously acts as NOO's substrate and strong inhibitory compound (Yarbrough *et al.* 1980), experiments using NOO and nitrite would provide fundamental insight into how the biostatic effect and biocidal effect take place in the system. In addition, if the nitrite toxicity (poisoning) of NOO is feasible in wastewater treatment processes, this biocidal effect might be also applied to develop new strategies for the suppression of NOO in nitritation processes (Wang *et al.* 2014).

Based on the background, living cell counting for NOO-enriched activated sludge was conducted in batch conditions with low to high nitrite concentrations. Together with the analysis of biomass concentration and the oxygen uptake rate (OUR) from the nitrite oxidation along with time, kinetic modelling nitrite toxicity of NOO was carried out. From the developed model, possibility to wash out NOO from the aeration tank was also discussed in this paper.

MATERIALS AND METHODS

Enrichment of NOO in the activated sludge

Nitrifying activated sludge was collected from a low-loaded membrane bioreactor treating domestic wastewater (Kitakyushu, Japan) with about 30-day sludge retention time (SRT) where intermittent aeration for nitrification and denitrification in the single tank was applied. The small amount of the nitrifying activated sludge was inoculated to 2 units of 5-L open jar fermenter equipped with a pH controller to keep pH = 7.0 and an external tubular ultrafiltration membrane module for the solid–liquid separation of activated sludge and effluent (X-Flow compact 0.17–5.2 MM, Pentair, USA) respectively. The activated sludge was continuously recycled between the jar fermenter and the membrane module with a diaphragm pump (APN-60GD2-W, Iwaki, Japan). In order to incubate different NOO cultures, one out of the two jar fermenters was operated under 25 °C with 200 mg-N/L of influent nitrite at 0.2-day of hydraulic retention time (HRT) and 40-days of SRT (reactor M), whilst the other was operated under 35 °C with 1,000 mg-N/L of influent nitrite at 2.0-day HRT and 80-days SRT (reactor H). The inorganic synthetic influent was made from sodium nitrite, phosphate buffer (0.4 mg-P/L), ammonium chloride (2.5 mg-N/L) and tap water. The dissolved oxygen concentrations and the effluent nitrite concentrations for both reactors were maintained to be about 5 mg-O_2/L and below 1–3 mg-N/L, respectively. After more than 1.5 years of the contentious operation, the NOO-enriched activated sludge was sampled from the reactors for batch experiments.

Live/dead microbial cell staining and microscopic observation

LIVE/DEAD® fixable green stain sampler kit L7012 (Thermo Fischer Scientific, USA) was used to visualise the living microbial cells in the NOO-enriched activated sludge samples. In principle, living cell was defined as a cell having undamaged cell membrane which was stained with green fluorescent reagent (Ex: 460–500 nm, Em: 515 nm), whereas cell having damaged cell membrane (non-green fluorescence) was defined as a dead cell (Lina *et al.* 1999). As the NOO-enriched activated sludge was slightly flocculated in both reactors, the sludge sample was preconditioned in order to disperse the flocs for the microscopic observation. For the pretreatment, the activated sludge was homogenised with an ultra-sonic cell disrupter (UD-200, Tomy, Japan). When ultrasonic homogenisation with 20 kHz at 18 W power input was applied for 30 s to the 10 mL of activated sludge sample in a 20 mL-test tube cooled with ice water, the number of visible cells stained in green colour was maximised. For the microscopic observation, the sample volume was also optimised to be 7.5 μL

on the glass slide with a square cover slip (256 mm^2). Too high a sample volume resulted in liquid leakage from the cover slip whilst too low liquid volume created imperfect air removal in the liquid zone between the cover slip and glass slide.

At 200 times of microscopic magnification (Eclipse 80i, Nikon, Japan), about 500 microscopic fields per glass slide which covered about 8% of the sample were recorded and digitalised with a binary image processor (Quick Grain, Inotech, Japan). Assuming that the area coloured in green per microscopic field area was proportional to the active biomass concentrations in the sample (Hao *et al.*, 2009), the growth and decay of the active biomass under presence of nitrite were evaluated.

Batch tests

Using the two kinds of NOO-enriched activated sludge, multisets of batch incubation tests were performed where the nitrite concentration in each incubation vessel was set to be 0, 25, 50, 100, 250, 500 and 1,000 mg-N/L for Reactor-M and 0, 25, 50, 100, 250, 500,750, 1,000 and 2,000 mg-N/L for Reactor-H, respectively. To maintain the nitrite concentration during the tests, a computer-programmed syringe pump (SP-2PC, As-one, Japan) was installed for continuous feeding high-strength sodium nitrite solution (20,000 mg-N/L) to the incubation vessel, which enabled to control the nitrite concentration within the target ± about 5%. Prior to the tests, the activated sludge samples were centrifugally washed three times with the inorganic synthetic wastewater excluding nitrite in order to ensure no nitrite was present in the samples. The washed activated sludge was mixed with the predetermined nitrite medium, and placed in each aerated 0.5-L incubation vessel where the water temperature during the 8-day experiments was kept to be the same as that in the reactor whilst the DO concentration was almost saturated to be about 8 mg-O_2/L with air. Small amount of sludge was sampled every day together whilst checking the nitrite concentration and pH in the incubation vessels. From the samples, visible living cells and particulate COD were measured. These batch incubation tests were carried out in a duplicate manner, and the dataplots of the two datasets were averaged.

For measuring NOO's OUR, the activated sludge in the incubation vessels was also manually sampled at 6–8-h intervals, and placed in a 100 mL Winkler bottle after precisely adjusting nitrite concentration to be the same as the predetermined concentration of each incubation vessel. The initial DO concentration of the sample was set to be beyond 10 mg-O_2/L using O_2 gas, and the DO consumption in the Winkler bottle was logged at every 1-min intervals with a potable DO meter (TOX-999B, Toko, Japan). Based on the decrement of DO concentration over time, the OUR of each incubation vessel was obtained.

Kinetic model

Model development

Considering that mixed cultures were cultivated in the open jar fermenters, besides the enriched NOO, a small amount of ordinary heterotrophic organism (OHO), ammonia oxidising organism (AOO) and unbiodegradable organic product from cell decay ($X_{U,Org}$) were expected to exist in the NOO-enriched activated sludge, which were generated from the decayed materials of NOO. Therefore, IWA Activated Sludge Model No. 1 (ASM1) having 'death–regeneration concept' that allowed to simulate the cryptic growth was chosen for the framework of modelling (Henze *et al.* 2000). For the model development, as shown in Table 1 ASM1 was modified to express two-step nitrification (ammonia to nitrite, and nitrite to nitrate) and nitrite toxicity on NOO. Although OHO and AOO might be also inactivated to a certain extent in the high nitrite concentration, these reactions were neglected in the model matrix for simplification.

The experimental datasets of the net specific growth rate were approximated with a composite rate equation consisted of terms for growth (μ) and total decay (b_{tot}) including nitrite toxicity as expressed in Equation (1). The switching function of the toxicity term was expressed with a sigmoid formula having a power coefficient ($n > 1$). Compared to the formula of conventional switching function ($n = 1$), this expression could create the curves close to the data plots as demonstrated in the Results and discussion section.

$$\begin{cases} r = \mu - b_{tot} \\ \mu = \mu_{\max,NO2}\left(\dfrac{S_{NO2}}{K_{NO2}+S_{NO2}}\right)\left(\dfrac{K_{I,NO2,gro}}{K_{I,NO2,gro}+S_{NO2}}\right) \\ b_{tot} = b + b_{NO2,tox}\left(\dfrac{S_{NO2}^{n}}{K_{I,NO2,tox}^{n}+S_{NO2}^{n}}\right) \end{cases} \quad (1)$$

where r: net specific growth rate from nitrite (d^{-1}), μ: specific growth rate from nitrite (d^{-1}), b_{tot}: total specific decay rate (d^{-1}), $\mu_{max,NO2}$: maximum specific growth rate from nitrite (d^{-1}), S_{NO2}: nitrite concentration (mg-N/L),

Table 1 | Model matrix of NOO's growth and decay with the cryptic growth of OHO and AOO in the system

Component → Process ↓	X_{NOO}	S_{O2}	S_{NO2}	S_{NO3}	$XC_{B,Org}$	$X_{U,Org}$	$S_{B,Org}$	$X_{CB,N}$	$X_{U,N}$	$S_{B,N}$	S_{NHx}	X_{OHO}	X_{AOO}	Process expression
Growth of nitrite oxidising organisms	1	$-(1.14/Y_{NOO}-1)$	$-1/Y_{NOO}$	$1/Y_{NOO}$							$-i_{N\_Bio}$			Monod type
Decay of nitrite oxidising organisms	−1				$1-f_{U\_Bio,lys}$	$f_{U\_Bio,lys}$		$(1-f_{U\_Bio,lys})\times i_{N\_Bio}$	$f_{U\_Bio,lys}\times i_{N\_Bio}$					First-order type
Nitrite poisoning for nitrite oxidising organisms	−1				$1-f_{U\_Bio,lys}$	$f_{U\_Bio,lys}$		$(1-f_{U\_Bio,lys})\times i_{N\_Bio}$	$f_{U\_Bio,lys}\times i_{N\_Bio}$					Sigmoid type
Hydrolysis of slowly biodegradable organic particulates					−1		1							Contois type
Hydrolysis of slowly biodegradable particulate nitrogen								−1		1				Contois type
Ammonification from biodegradable soluble nitrogen										−1	1			First-order type
Cryptic growth of ordinary heterotrophic organism		$-(1/Y_{OHO}-1)$					$-1/Y_{OHO}$				$-i_{N\_Bio}$	1		Monod type
Cryptic growth of ammonium oxidising organism		$-(3.43/Y_{AOO}-1)$	$1/Y_{AOO}$								$-i_{N\_Bio}-1/Y_{AOO}$		1	Monod type
Decay of ordinary heterotrophic organism					$1-f_{U\_Bio,lys}$	$f_{U\_Bio,lys}$		$(1-f_{U\_Bio,lys})\times i_{N\_Bio}$	$f_{U\_Bio,lys}\times i_{N\_Bio}$			−1		First-order type
Decay of active ammonium oxidising organism					$1-f_{U\_Bio,lys}$	$f_{U\_Bio,lys}$		$(1-f_{U\_Bio,lys})\times i_{N\_Bio}$	$f_{U\_Bio,lys}\times i_{N\_Bio}$				−1	First-order type
	Nitrite oxidising organism (mg-COD/L)	Dissolved oxygen ($mg\text{-}O_2/L$)	Nitrite (mg-N/L)	Nitrate (mg-N/L)	Slowly biodegradable organic particulates (mg-COD/L)	Unbiodegradable organic particulates from cell decay (mg-COD/L)	Readily biodegradable soluble organics (mg-COD/L)	Slowly biodegradable nitrogenous particulates (mg-COD/L)	Unbiodegradable nitrogenous particulates from cell decay (mg-N/L)	Readily biodegradable soluble nitrogen (mg-N/L)	Free and ionised ammonia (mg-N/L)	Ordinary heterotrophic organism (mg-COD/L)	Ammonia oxidising organism (mg-COD/L)	

K_{NO2}: half-saturation coefficient of nitrite on growth (mg-N/L), $K_{I,NO2,gro}$: half-saturation coefficient of nitrite on growth inhibition (mg-N/L), b: inherent specific decay rate (d^{-1}), $b_{NO2,tox}$: specific nitrite toxicity rate (d^{-1}), $K_{I,NO2,tox}$: half-saturation coefficient of nitrite on toxicity (mg-N/L), n: power coefficient of nitrite toxicity (–).

Model solution procedure

In this study, NOO-relating parameters were the focused because the other active biomass fractions (OHO and AOO) in the NOO-enriched activated sludge were supposed to be relatively minor. In order to estimate the NOO-relating parameters for $\mu_{max,NO2}$, b, $b_{NO2,tox}$, $K_{I,NO2,tox}$ and n, the increment/decrement of visible green-coloured cell areas against time were analysed. Besides the analysis, additional measurement for $K_{I,NO2,gro}$ and K_{NO2} was conducted in another batch experiment where OUR of the NOO-enriched activated sludge was measured with a Winkler bottle under various nitrite concentrations. From the OUR dataplots and curve fitting, $K_{I,NO2,gro}$ and K_{NO2} were accurately determined.

Next, in order to know each biomass concentration in the reactors, adopting the biomass yield coefficients, production of particulate inert, kinetics for hydrolysis, ammonification, AOO growth/decay and OHO growth/decay from literature (Chandran & Smeths 2000; Henze *et al.* 2000; GPS-X technical reference 2012; Makinia 2010), a steady-state calculation of each reactor was conducted under the fixed SRT and volumetric loading rate. Based on the calculated biomass concentrations, the particulate COD concentrations and the OURs in the batch incubation tests were dynamically simulated and compared with the dataplots assuming that only NOO was inhibited by nitrite. To complete the calibration over the visible green-coloured cell areas, the particulate COD concentrations and the OURs, some parameters (biomass yield coefficients and specific decay rates) were slightly manipulated. These calibrated kinetic and stoichiometric parameters were summarised in Table 2.

From the above calibration, the COD-based biomass fractions of the NOO-enriched activated sludge in the reactors were obtained in the followings; Reactor-M: NOO = 71.1%, OHO = 5.6%, AOO = 0.6%, $X_{U,Org}$ = 22.7%, Reactor-H: NOO = 57.9%, OHO = 9.4%, AOO = 0.1%, $X_{U,Org}$ = 32.6%. In both reactors, about 86–90% of active biomass seemed to be accounted for NOO, and the rest of 10–14% was mostly composed of OHO. AOO fraction was very minor in the active biomass due to low yield coefficient.

Analytical methods

Particulate COD of the washed NOO-enriched activated sludge in the reactors was measured using COD analysis kit (TNT Plus 821 (COD range 3–150 ppm), HACH, USA). Nitrite concentration was obtained using an ion chromatography system equipped with Ion Pac AS11-HC column (ICS-1000, Thermo Fisher Scientific Inc., USA) where the elute flow rate was set to be 1 mL/min at 35 °C with 4 mol/L of KOH solution. A process simulator (GPS-X ver. 6.4, Hydromantis, Canada) was used to simulate the particulate COD concentrations and OUR on the modified ASM1.

RESULTS AND DISCUSSION

Nitrite toxicity on NOO

As shown in the top left graph of Figure 1(a), when the activated sludge taken from Reactor-M was exposed to nitrite beyond 100 mg-N/L, the visible living cell area decreased along with time. The decrease was accelerated in the incubation vessels containing more than 250 mg-N/L of nitrite, and was faster than that of the control incubation vessel without addition of nitrite. From the accelerated decrease of the visible living cell area, nitrite toxicity was experimentally recognised. In the experimental condition, the visible living cell area was only increased when the nitrite concentration was set to be less than 50 mg-N/L. As the elevation of the visible living cell area with 50 mg-N/L of nitrite was slower than that with 25 mg-N/L, growth inhibition under high nitrite concentration was also recognised in the test.

Since the decrease/increase of the visible living cell area versus the incubation time seemed to be expressed in exponential manner, a semi-logarithmic regression was performed and each slope (=net specific growth rate = μ–b_{tot}) was plotted on the basis of the nitrite concentration in the incubation vessel. As shown in the top right graph of Figure 1(b), it appeared that the net specific growth rate peaked at about 25 mg-N/L of nitrite, and reached zero at about 60 mg-N/L of nitrite. Beyond the nitrite concentration, the net specific growth rate became negative leading to a decrease of the active biomass concentration in time. At 1,000 mg-N/L of nitrite, about $-0.3\ d^{-1}$ of net specific growth rate was obtained.

With respect to the activated sludge taken from Reactor-H, as shown in the bottom left graph of Figure 1(c), toxicity and growth inhibition by nitrite was also observed.

Table 2 | Model parameters for NOO's growth and decay with the cryptic growth of OHO and AOO in the system

Parameters		Reactor-M	Reactor-H	Reference
NOO-relating parameters				
Max. specific growth rate (d^{-1})	$\mu_{NOO,\ max,NO2}$	0.21	0.19	♣
Half-saturation coefficient of nitrite on growth (mg-N/L)	$K_{S,NO2,NOO}$	0.5	10	♣
Half-saturation coefficient of nitrite on growth inhibition (mg-N/L)	$K_{I,,NO2,gro,NOO}$	70	520	♣
Inherent specific decay rate (d^{-1})	b_{NOO}	0.050	0.076	♣
Max. specific nitrite toxicity rate (d^{-1})	$b_{NO2,tox,NOO}$	0.3	0.25	♣
Half-saturation coefficient of nitrite on toxicity (mg-N/L)	$K_{I,NO2,to,NOO}$	180	720	♣
Power coefficient of substrate toxicity (dimensionless)	n	5	5	♣
Biomass yield coefficient (g-COD/g-N)	Y_{NOO}	0.06	0.06	♦
OHO-relating parameters				
Max. specific growth rate (d^{-1})	$\mu_{OHO,max}$	6.0	← ditto	♥
Half-saturation coefficient of organic substrate (mg-COD/L)	$K_{S,OHO}$	20	← ditto	♥
Specific decay rate (d^{-1})	b_{OHO}	0.62	← ditto	♥
Max. specific hydrolysis rate (d^{-1})	$q_{OHO,Max,XCB}$	3.0	← ditto	♥
Half-saturation coefficient of hydrolysis (dimensionless)	K_{XCBorg_OHO}	0.1	← ditto	♥
Specific ammonification rate (L/mg-COD/d)	$q_{OHO,XCB,N}$	0.08	← ditto	♥
Biomass yield coefficient (g-COD/g-COD)	Y_{OHO}	0.666	← ditto	♥
AOO-relating parameters				
Max. specific growth rate (d^{-1})	$\mu_{AOO,max}$	0.26	← ditto	♦
Half-saturation coefficient of ammonia on growth (mg-N/L)	$K_{S,NHx,AOO}$	1.0	← ditto	♥
Specific decay rate (d^{-1})	b_{AOO}	0.06	← ditto	♣
Biomass yield coefficient (g-COD/g-N)	Y_{AOO}	0.208	← ditto	♦
Global parameters				
Fraction of inert organics in biomass (g-COD/g-COD)	$f_{XU\_Bio,lys}$	0.08	← ditto	♥
Nitrogen content of biomass (g-N/g-COD)	i_{N_Bio}	0.086	← ditto	♥

♣ This study, ♦ Adopted from Chandran & Smeths (2000), Makinia (2010) and GPS-X technical reference (2012), ♥ Henze *et al.* (2000).

However, the tolerance against nitrite was distinct from that of Reactor-M. The visible living cell area increased even at 250 mg-N/L of nitrite, and toxicity was not recognised until the nitrite concentration was set at 750 mg-N/L. As shown in the bottom right graph of Figure 1(d), the nitrite threshold of Reactor-H where the net specific growth rate dropped to zero was estimated to be about 400 mg-N/L, and the net specific growth rate eventually reached about $-0.25\ d^{-1}$.

For kinetic modelling, besides the above nitrite threshold leading the net specific growth rate to zero, the half-saturation coefficient of nitrite on toxicity ($K_{I,NO2,tox}$) could be defined as an alternative index to express the degree of toxicity because the power coefficient ($n = 5$) of the sigmoid formula was large enough to immediately switch the ordinary decay (b) to the decay with poisoning ($b + b_{NO2,tox}$) around the nitrite concentration. On the other hand, lethal dose of nitrite ($S_{NO2,LD50}$) to reduce NOO biomass by 50% at time = T might be also expressed in Equation (2), which was derived from from Equation (1), whereas the formula of b_{tot} should be inhibitor and species specific.

$$\begin{cases} 50\% = \exp(-b_{tox} \times T) \\ b_{tox} = b_{NO2,tox}\left(\dfrac{{S_{NO2,LD50}}^n}{{K_{I,NO2,tox}}^n + {S_{NO2,LD50}}^n}\right) \end{cases} \quad (2)$$

Dynamic simulation of OUR and COD concentration

As shown in Figure 2, the dynamic simulation could fairly reproduce both measured OURs and COD concentrations.

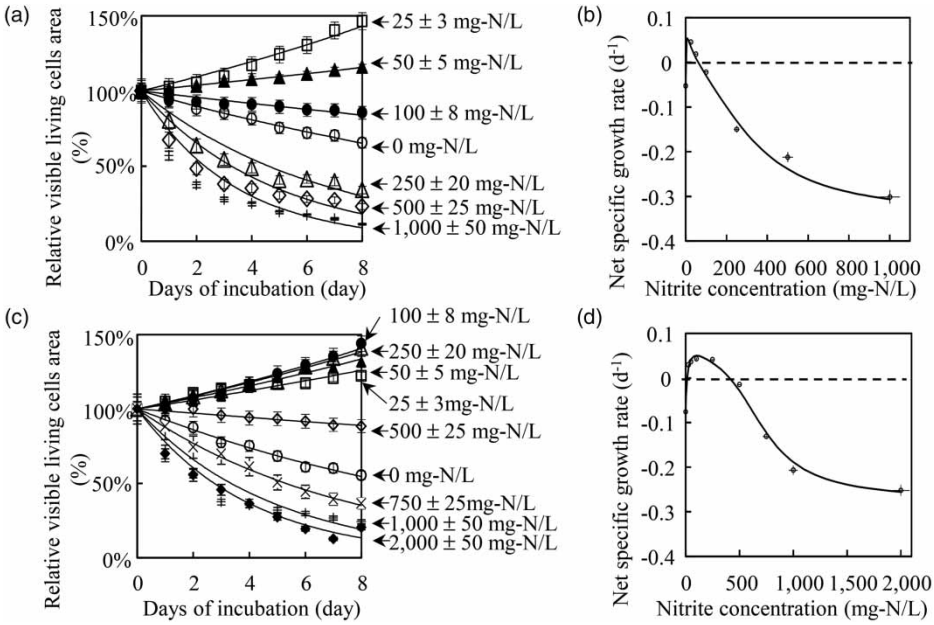

Figure 1 | Nitrite toxicity on nitrite oxidising organisms. (a) and (b) Reactor-M; (c) and (d) Reactor-H; left: visible living cell area with 95% confidence interval vs. incubation time; right: net specific growth rate with 95% confidence interval vs. nitrite concentration; plot: experiment; line: regression.

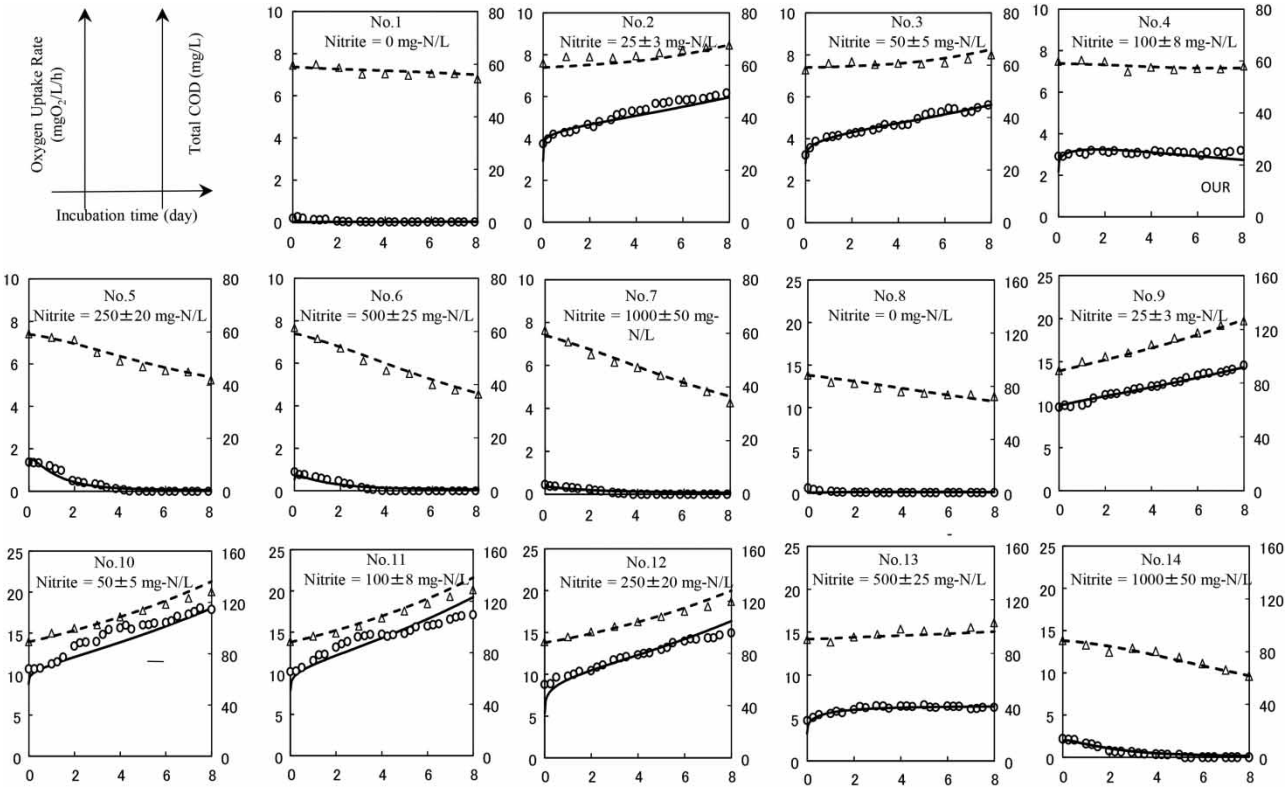

Figure 2 | Responses of OUR and particulate COD concentration in the batch tests. #1–7: Reactor-M; #8–14: Reactor-H; ○: OUR; △: COD; line: simulation.

For Reactor-M, both OUR and COD with 25 mg-N/L of nitrite responded to increase along with time. The increase was also recognised in the incubation vessel with 50 mg-N/L of nitrite, whereas OUR was almost kept constant when 100 mg-N/L of nitrite was present. This stagnation of OUR was consistent with the poor growth of visible living cell area over the incubation period. The slight decrease of COD at 100 mg-N/L of nitrite was due to the endogenous decay of OHO in the activated sludge, which was also seen in the blank test without addition of nitrite. Beyond 250 mg-N/L of nitrite, both OUR decay and COD decay became noticeable, indicating that biomass lysis of NOO took place in the conditions. When the nitrite concentration was doubled to 500 mg-N/L, the decreases of OUR and COD were accelerated. In case of 1,000 mg-N/L of nitrite, only trace OUR was observed over the experimental period. For Rector-H, both OUR and COD increased along with time when the nitrite was kept at 25 mg-N/L, 50 mg-N/L, 100 mg-N/L and 250 mg-N/L, respectively. At 500 mg-N/L of nitrite, the system responded to be a marginal growth of OUR and COD. The biomass lysis and the nitrite toxicity for Reactor-H were only recognised when nitrite concentration was set to be beyond 750 mg-N/L.

The maximum specific growth rates of NOO obtained in this study (Reactor-M: 0.21 d^{-1}, Reactor-H: 0.19 d^{-1}) were considerably lower than those in literature ($\mu_{NOO,\,max,NO2}$ = 0.28–3.0 d^{-1}) (Knowles *et al.* 1965; Wyffels *et al.* 2004; Makinia 2010), whilst the specific decay rates (Reactor-M: 0.05 d^{-1}, Reactor-H: 0.076 d^{-1}) were comparable to those summarised by Makinia (2010) (b_{NOO} = 0.03–0.06 d^{-1}). For the half-saturation coefficient of nitrite on growth, the kinetic value of Reactor-H was 20 times as high as that of Reactor-M ($K_{S,NO2,NOO:}$ 10 mg-N/L vs. 0.5 mg-N/L). Compared to the NOO in Reactor-H, the NOO in Reactor-M seemed to have considerably lower tolerance against nitrite for both toxicity and growth inhibition. In fact, the calibrated half-saturation coefficient on nitrate toxicity of Reactor-M was much lower than that of Reactor-H ($K_{I,NO2,po}$: 180 mg-N/L vs. 720 mg-N/L) as well as low half-saturation coefficient on growth inhibition ($K_{I,No2,gro}$: 70 mg-N/L vs. 520 mg-N/L). Although exact cause to yield NOOs having distinct tolerance against nitrite was not clear, the incubation temperature (25 °C vs. 35 °C), salinity derived from the influent sodium nitrite (200 mg-N/L vs. 2,000 mg-N/L) and/or SRT (40-days vs. 80-days) might be the factors. Therefore, in order to control NOO growth in nitritation processes, operating conditions not to accumulate high tolerance NOO in the aeration tank should be explored and clarified in future studies.

Possibility to suppress growth of NOO with nitrite toxicity

If nitrite concentration in a continuous bioreactor exceeded the toxicity threshold, NOO could not be retained even if the system had long SRT. Therefore, the nitrite toxicity phenomena might be utilised as an alternative method to reduce NOO biomass in the AB process (de Graaff *et al.* 2016). For instance, as illustrated in Figure 3, when a part of return activated sludge in the B-stage was mixed with high nitrite liquor in the side-stream partial nitritation reactor, significant amount of the NOO in the activated sludge would be irreversibly inactivated if the SRT in the partial nitritation reactor was long enough. In this case, since the side-stream partial nitritation reactor could act as a selector to remove NOO from the B-stage, this process configuration might push to wash out NOO from the B-stage aeration tank, which helped to maintain main stream partial nitritation and Anammox processes.

To evaluate the possibility, critical nitrite toxicity condition of the selector to wash out NOO was deduced. The B-stage aeration tank was modelled to receive the influent

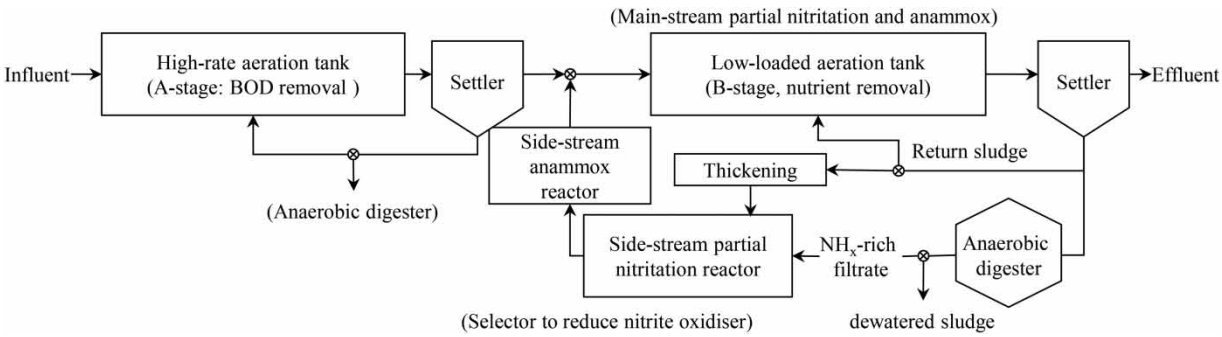

Figure 3 | Possible scheme to reduce the growth of NOO in the aeration tank.

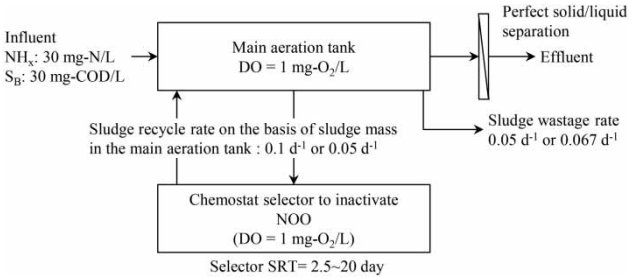

Figure 4 | Simulation boundary of NOO washout using selector.

composed of 30 mg-COD/L of organic substrate and 30 mg-N/L of ammonium-N, respectively, where the excess sludge was withdrawn at either 0.05 d^{-1} (SRT = 20 d) or 0.067 d^{-1} (SRT = 15 d) of sludge wastage rate θ_M. To perform steady-state simulations, NOO kinetics in the aeration tank were assumed to be $\mu_{NOO,max} = 0.3\ d^{-1}$, $K_{S,NO2,NOO} = 0.5$ mg-N/L, $K_{O2,NOO} = 0.72$ mg-O_2/L and $b_{NOO} = 0.05\ d^{-1}$, and the half-saturation coefficients of oxygen for OHO and AOO were additionally defined to be $K_{O2,AOO} = 0.30$ mg-O_2/L and $K_{S,O2,OHO} = 0.45$ mg-O_2/L, respectively (GPS-X technical reference 2012). Due to long SRT in the system, the impact of the above growth-relating parameter values on the effluent quality were limited (calculation not shown). The selector was modelled to be a chemostat tank. The activated sludge in the main aeration tank was recycled to the selector at either 0.05 d^{-1} or 0.1 d^{-1} of the internal recycle rate θ_S. Since the NOO retention time in the selector (selector SRT) was one of the operational factors for NOO washout as well as θ_M and θ_S. The selector SRT was varied in 0–20 days under two scenarios of the sludge flow rate (scenario A: $\theta_M = 0.05\ d^{-1}$, $\theta_S = 0.1\ d^{-1}$; scenario B: $\theta_M = 0.067\ d^{-1}$, $\theta_S = 0.05\ d^{-1}$). The simulation boundary was illustrated as shown in Figure 4. Both reactors were operated under 1.0 mg-O_2/L of dissolved oxygen.

Considering that the toxicity coefficients on NOO ($b_{NO2,tox}$ and $K_{I,NO2,tox}$) were not consistent over the two NOO-enriched activated sludge, total specific decay rate of NOO ($b_{tot,NOO}$, variable) in the selector was externally given to the the steady-state simulations. By changing the the parameter value, the critical $b_{tot,NOO}$ to attain NOO wash-out was identified. To reduce model complexity, partial nitritation by AOO in the selector was not introduced to the calculation. Instead, as mentioned above, slightly high ammonium-N concentration was applied to the influent for maintaining AOO biomass in the entire system.

As shown in the left graph of Figure 5 (Scenario A), the main aeration tank without selector yielded about 90% of nitrate conversion efficiency, whereas the modified process equipped with the selector could produce nitrite with more than 90% of conversion efficiency when $b_{tot,NOO}$ was high enough. The critical $b_{tot,NOO}$ depended on the selector SRT. When the selector SRT was shortened, high $b_{tot,NOO}$ was needed to wash out NOO from the system. As 0.25–0.3 d^{-1} of maximum specific nitrite toxicity rate ($b_{NO2,tox}$) for NOO and 0.05 d^{-1} of inherent specific decay rate for NOO (b_{NOO}) were obtained in this study, attainable $b_{tot,NOO}$ might be utmost about 0.30–0.35 d^{-1} (=b_{NOO} + $b_{NO2,tox}$). Hence, very short selector SRT which required beyond 0.30–0.35 d^{-1} of $b_{tot,NOO}$ would not be feasible. In the scenario, 5-day selector SRT was in the attainable range whereas 2.5-day selector SRT could not meet the criterion.

As shown in the right graph of Figure 4 (scenario B), the critical $b_{tot,NOO}$ on each selector SRT shifted upward. In this scenario, about 7.5-day selector SRT was the marginal operating condition to meet the criterion for upper limit of $b_{tot,NOO}$. The reason to require higher system SRT than that of scenario A was accounted for its high θ_M and low θ_S (high growth rate of NOO in the main aeration tank).

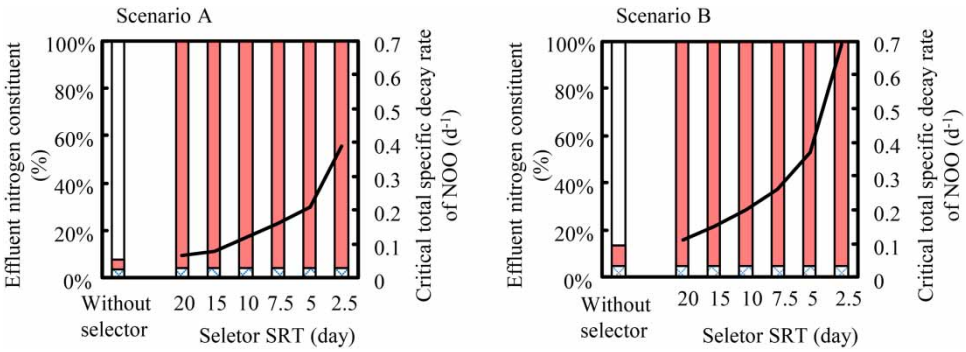

Figure 5 | Critical nitrite poisoning conditions at the selector to wash out NOO from the main aeration tank. Left: scenario A, activated sludge wastage rate from the aeration tank = 0.05 d^{-1}, activated sludge recycle rate between the B-stage and the selector = 0.1 d^{-1}; right: scenario B, activated sludge wastage rate from the aeration tank = 0.067 d^{-1}; activated sludge recycle rate between the B-stage and the selector = 0.05 d^{-1}; ⊠: ammonium-N; ■: nitrite-N; □: nitrate-N; line: critical total specific decay rate of NOO.

Nevertheless, the selector volume ($=\theta_S \times$ selector SRT) of scenario B could be reduced by 25% comparing to that of scenario A (scenario A : scenario B = 0.5 : 0.375). Since the kinetic parameters for NOO would be site-specific as demonstrated in the experiments using Reactor-M and Reactor-H, these parameters should be measured in each wastewater treatment plant. The selector volume, the marginal conditions for θ_S and selector SRT and $b_{tot,NOO}$ in the selector could be further lowered if the other options to reduce specific NOO growth rate in the main aeration tank was also applied (e.g. low DO set point).

CONCLUSION

Nitrite toxicity was examined for nitrifying activated sludge using two kinds of NOO-enriched culture. From the study the following results were obtained.

1. Nitrite was found to give an irreversible decay for the biological nitrite oxidation. At higher nitrite concentration, higher specific decay rate leading to nitrite toxicity was recognised.
2. The specific toxicity rate of nitrite was expressed as a first-order reaction on the basis of NOO concentration (about 0.25–0.30 d^{-1}) having a sigmoid switching function for nitrite.
3. The tolerance of the nitrite toxicity was highly dependent on the culture. The culture incubated under 25 °C did not grow when 60 mg-N/L of nitrite was present whilst the other incubated under 35 °C could grow even under 400 mg-N/L of nitrite.
4. From the mathematical simulation, NOO seemed to be washed-out from the mainstream aeration tank when the microorganism was exposed to high nitrite for a certain period of time in the side-stream partial nitritation reactor.

ACKNOWLEDGEMENTS

This work was supported by Japan Society for the Promotion of Science. The authors sincerely thank Ms Ren Hong for her great contribution to the experiments.

REFERENCES

Anthonisen, A. C., Loehr, R. C., Prakasam, T. B. S. & Srinath, E. G. 1976 Inhibition of nitrification by ammonia and nitrous acid. *Journal of the Water Pollution Control Federation* **48** (5), 835–852.

Batstone, D. J., Keller, J., Angelidaki, I., Kalyuzhnyi, S. V., Pavlostathis, S. G., Rozzi, A., Sanders, W. T. M., Sirgrist, H. & Vavilin, V. A. 2002 *Anaerobic Didestion Model No. 1. IWA Scientific and Technical Report No. 13*, London, UK.

Calderer, M., Jubanya, I., Pérez, R., Martí, V. & de Pablo, J. 2010 Modelling enhanced groundwater denitrification in batch microcosm tests. *Chemical Engineering Journal* **165**, 2–9.

Chandran, K. & Smeths, F. S. 2000 Single-step nitrification models erroneously describe batch ammonia oxidation profiles when nitrite oxidation becomes rate limiting. *Biotechnology and Bioengineering* **68** (4), 396–406.

Chen, Z., Wang, X., Yang, Y.-Y., Mirino Jr., M. W. & Yuan, Y. 2016 Partial nitrification and denitrification of mature landfill leachate using a pilot-scale continuous activated sludge process at low dissolved oxygen. *Bioresource Technology* **218**, 580–588.

David, S. P. & Peter, R. J. 2016 Modeling the inhibition of dissolved H_2 on propionate fermentation and methanogenesis in wetland sediments. *Ecological Modelling* **322**, 115–123.

de Graaff, M. S., van den Brand, T. P. H., Roest, K., Zandvoort, M. H., Duin, O. & van Loosdrecht, M. C. M. 2016 Full-scale highly-loaded wastewater treatment processes (A-stage) to increase energy production from wastewater: performance and design guidelines. *Environmental Engineering Science.* **33** (8), 571–577.

GPS-X technical reference 2012 Hydromantis Inc., Hamilton, Ontario, Canada.

Hao, X., Wang, Q., Zhang, X., Cao, Y. & van Loosdrecht, M. C. M. 2009 Experimental evaluation of decrease in bacterial activity due to cell death and activity decay in activated sludge. *Water Research* **43**, 3604–3612.

Henze, M., Gujer, W., Mino, T. & van Loosdrecht, M. C. M. 2000 *Activated Sludge Models ASM1, ASM2, ASM2d, and ASM3. IWA Scientific and Technical Report No. 9*, London, UK.

Knowles, G., Downing, A. L. & Barrett, M. J. 1965 Determination of kinetic constants for nitrifying bacteria in mixed culture, with the aid of electronic computer. *Journal of General Microbiology* **38**, 263–278.

Lina, B., Michele, P., Benoit, B., Josee, C. & Raymond, D. 1999 LIVE/DEAD® BacLight™: application of a new rapid staining method for direct enumeration of visible and total bacteria in drink water. *Journal of Microbiological Methods* **37**, 77–86.

Liu, B., Jarvis, I., Naka, D., Goel, R. & Yasui, H. 2013 A benchmark simulation to verify an inhibition model on decay stage for nitrification. *Water Science and Technology* **68** (6), 1242–1250.

Makinia, J. 2010 *Mathematical Modelling and Computer Simulation of Activated Sludge Systems*. IWA Publishing, London, UK.

Manser, R., Gujer, W. & Siegrist, H. 2006 Decay processes of nitrifying bacteria in biological wastewater treatment systems. *Water Research* **40**, 2416–2426.

Wallenstein, M. D., Myrold, D. D., Firestone, M. & Voytek, M. 2006 Environmental controls on denitrifying communities

and denitrification rates: insights from molecular methods. *Ecological Applications* **16**, 2143–2152.

Wang, Q., Liu, Y., Jiang, G., Hu, S. & Yuan, Z. 2014 Side-stream sludge treatment using free nitrous acid selectively eliminates nitrite oxidizing bacteria and achieves the nitrite pathway. *Water Research* **55**, 245–255.

Weibull, W. 1952 A statistical distribution function of wide application. *ASME Journal of Applied Mechanics* **September**, 293–297.

Wett, B. & Rauch, W. 2003 The role of inorganic carbon limitation in biological nitrogen removal of extremely ammonia concentrated wastewater. *Water Research* **37**, 1100–1110.

Wu, J., He, C., van Loosdrecht, M. C. M. & Pére, J. 2016a Selection of ammonium oxidizing bacteria (AOB) over nitrite oxidizing bacteria (NOB) based on conversion rates. *Chemical Engineering Journal* **304**, 953–961.

Wu, J., Zhang, Y. & Yan, G. 2016b Differentiating two partial nitrification mechanisms: inhibiting nitrite oxidizing bacteria activity or promoting ammonium oxidizing bacteria activity. *Journal of Environmental Chemical Engineering* **4**, 3260–3266.

Wyffels, S., Van Hulle, S. W. H., Boeckx, P., Volcke, E. I. P., Van Cleemput, O., Vanrolleghem, P. A. & Verstraete, W. 2004 Modeling and simulation of oxygen-limited partial nitritation in a membrane-assisted bioreactor (MBR). *Biotechnology and Bioengineering* **86** (5), 531–542.

Yarbrough, J. M., Rake, J. B. & Eagon, R. G. 1980 Bacterial inhibition effects of nitrite: inhibition of active transport, but not of group translocation, and of intracellular enzymes. *Applied and Environmental Microbiology* **3** (9), 831–834.

First received 20 February 2018; accepted in revised form 5 June 2018. Available online 15 June 2018